APPLIED RESEARCH

Toward Controlling Transtibial Prostheses Using a Single Degree of Freedom Inertial Sensor System

ANIKET MAZUMDER [1], **EDSKO E. G. HEKMAN** [2], **(Member, IEEE),**
AND RAFFAELLA CARLONI [1], **(Senior Member, IEEE)**

[1]Faculty of Science and Engineering, Bernoulli Institute for Mathematics, Computer Science and Artificial Intelligence, University of Groningen, 9747 AG Groningen, The Netherlands
[2]Department of Biomechanical Engineering, Faculty of Engineering Technology, University of Twente, 7522 NB Enschede, The Netherlands

Corresponding author: Aniket Mazumder (a.mazumder@rug.nl)

ABSTRACT Control strategies for lower limb prostheses have made multiple significant advancements over the years. In this work, we investigate the scope and capabilities of a controller for ankle-foot prostheses that relies only on a one-degree-of-freedom inertial sensor, supplemented with a control algorithm that can perform a real time update of actuation parameters using gait information available from past gait cycles. The updated actuation parameters are applied to the subsequent gait cycle and the cycle repeats itself. The idea behind this controller is to allow a user to have infinite possible variations in gait speeds (within the allowable limits of actuation) while keeping the required sensory inputs to a minimum. As a consequence of this controller design, the user is not forced to choose discrete speeds of walking (slow, medium, fast) and is capable of freely varying his gait speeds on each step, while utilizing only a single-degree-of-freedom sensor. We implement the controller on an actuated transtibial prosthesis prototype based on a series-elastic spring configuration, and conduct tests for level ground walking at a self-selected walking speed, to explore the achievable range of response pertaining to daily living tasks. The pilot tests on a healthy participant, conducting level ground walking with turns and remotely controlling the prosthesis, suggest that it is possible to control a transtibial prosthesis using a simple uni-sensor framework, with a maximum angular deviation of $5°$, and maximum deviation in angular velocity of $20°/s$ compared to that of healthy humans.

INDEX TERMS Prosthetics, rehabilitation robotics, control design.

I. INTRODUCTION

The restoration of mobility for lower-limb amputees is a primary challenge for rehabilitation researchers. A solution to mobility following an amputation has been to use prosthetic systems that enable amputees to perform their daily activities albeit with some limitations. Usually, prosthetic systems are built to provide passive support [1], [2], however, prostheses with an active push-off capability have also been extensively researched [3], [4], [5].

The associate editor coordinating the review of this manuscript and approving it for publication was Giulio Reina [ ].

Active prostheses incorporate sensors that provide feedback to the prosthesis controller, which regulates an actuator. The controller's functionality revolves around determining the current gait state and formulating a suitable real-time response strategy. Several approaches detailing this process can be found in the literature [6]. The prominent ones, namely finite-state impedance control, volitional control, echo control, and electromyographic-based control methods, are described below.

The finite-state-based impedance control strategy is a widely used method for prosthesis control. As demonstrated in several studies, including [7], [8], [9], and [10], the entire

gait cycle is first divided into multiple states, with transition strategies for walking, standing, sitting, etc. An intent recognizer analyzes sensor data to determine the gait state, which is then classified using probabilistic models. Impedance, which matches the joint impedance of healthy human joints, is then mapped onto the prosthesis and used in gait state transitions. Imparting joint torques instead of using a high-gain position controller directly for actuation provides a more natural feel to the prosthesis user [11], [12].

Another approach to the control problem is the use of a gait phase determination algorithm, also known as volitional control, as demonstrated in studies such as [13], [14], and [15]. In this method, devices that measure rotation rate, such as gyroscopes or potentiometers, are placed on the residual limb segment. Integration of the rate of rotation provides the angles of the segment with respect to the gravity vector. To avoid errors in integration, transfer functions or recursive filters are used [16], [17]. A phase relation correlating limb-segment angular velocity and the segment angle is then determined. Utilizing this relation, the walking velocity and joint angles during walking can be directly determined. Additional sensors, such as a force/load sensor, are often used to supplement these methods for heel-off and heel-contact determination and for more accurate actuation timing [18].

A third approach is the echo control method [19], [20], where the sound limb motion is used as a reference motion profile for the prosthetic limb. This control method is suitable for repetitive tasks, such as walking on treadmills, but its performance decreases rapidly beyond laboratory conditions because sound limb compensation motions cannot be directly translated into raw motion profiles for the prosthetic limb in all scenarios. Instrumentation of the sound leg can also impede the movement of the prosthesis' user.

Another popular approach is the control of prostheses by using electromyographic (EMG) signals as shown in, e.g., [21], [22], and [23]. EMG signals are classified using machine learning models, and a real-time intent detector can be designed [13]. Since the accuracy of classifiers ranges from 95% to 99%, myoelectric control mechanisms are also often supplemented with kinematic/inertial sensors to improve accuracy and ensure proper detection of gait states. EMG control methods also suffer from instrumentation difficulties [24], [25], such as maintaining proper sensor-to-skin contact, signal filtering and noise rejection, making them difficult to be use in commercial prosthetic systems.

Besides the aforementioned control strategies, few other methods have been used to a lesser extent, such as controller based on intent recognition using eye motion [26], on the movement pattern of the hip [27], on gait phase synchronization using an adaptive oscillator [15], [28], [29], on fuzzy logic by using a combination of a potentiometer at the knee joint and an accelerometer at the femur [30], [31].

The primary motivation of the above-mentioned studies has been to achieve a satisfactory level of control functionality for a prosthetic system through the use of as many sensors as necessary. Since relying on multiple sensors inherently involves dealing with multiple control parameters along with the possibility of multiple sensor failures, there is a scope for a study to determine control performance with a limited number of sensors. In [32] and [33], multi-DOF (degrees of freedom) inertial sensors in combination with contact sensors/load cells performed optimally in a range of activities such as level-ground walking, ramp ascent/decent, walking at brisk speeds, etc. On the other hand, in [17], [34], and [35], it was shown that there exists a relation between the shank angular velocity and shank angular position such that a gait phase variable can be generated by relating both parameters.

Utilizing this knowledge, in this study, we explore the scope and possibility of designing a control architecture, that utilizes only a single sensor axis (specifically, a gyroscope with a single axial DOF) to control a transtibial prosthesis by relating the angular velocity of the tibia in the sagittal plane with the ankle joint angle (without requiring them to be directly linked through a continuously varying gait phase variable), and yet allows for an infinite possible combinations of gait speeds between two gait cycles. Usually in controllers with limited sensory inputs, the speed choices are limited to slow, medium and fast walking [33]. The controller implemented here goes around this limitation by using standard gait speeds from [36], and combining it with the step time information of the previous gait cycle.

Although, generally, Inertial Measurement Units (IMUs) come as a combination of a triple-axis accelerometer, gyroscope, and magnetometer, no other sensory inputs except a single axis of a gyroscope is to be used in this proposed method. The objective of the study is, thus, to determine whether a singular-axis inertial sensor is sufficiently capable of controlling a transtibial prosthesis for level ground walking with speed variations. The extent and limits of functionality achievable using such a controller are determined by implementing and testing it at preferred walking speed on a prosthetic prototype that has been specifically designed for this study.

The remainder of the paper is organized as follows. The mechanical design requirements and the prosthesis design are discussed in Section II. The control requirements along with the design of the control system are presented in Section III. Experiments with the prosthesis and the results are shown in Sections IV and V, respectively. Discussions and refinements are presented in Section VI, while limitations are mentioned in Section VII. Finally, concluding remarks are drawn in Section VIII.

II. MECHANICAL DESIGN

This section presents the mechanical design of the transtibial prosthesis that has been realized to validate the control architecture proposed in this study. The design requirements and the choice of components are described hereafter.

A. DESIGN REQUIREMENTS

The mechanical design requirements for the transtibial prosthesis have been established based on biomechanical data of healthy human subjects for level ground walking [36]. Figure 1 illustrates the ranges of ankle joint motion, torque, and power of a healthy human ankle during normal walking [36]. Therefore, an ankle prosthesis must offer a minimum angular range of 20° plantarflexion and 10° dorsiflexion, along with peak torques of 1.5-1.8 Nm/kg and power output of 4-4.5 W/kg. Moreover, an ankle prosthesis must meet the following three functional requirements: (i) After initial ground contact, a plantar-flexed ankle must be capable of dorsiflexion during roll-over, followed by a smooth powered push-off. (ii) Following the powered push-off accompanied by a plantarflexion, the ankle must be able to return to a neutral/dorsiflexed position for a swing phase toe clearance. (iii) A neutral/dorsiflexed ankle at the end of the swing must be capable of plantar flexion and absorb the impact of the heel-to-ground contact.
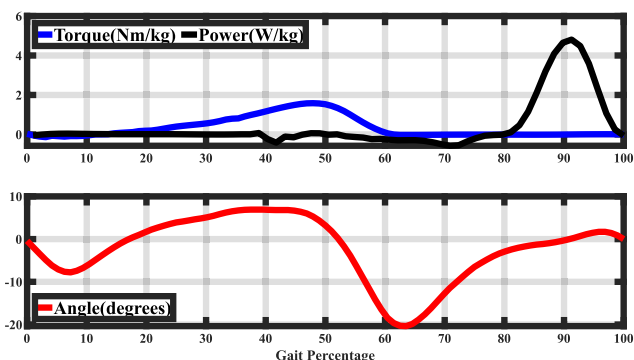

FIGURE 1. Ranges of ankle joint angle, torque, and power during normal level ground walking for a healthy subject [36].

To achieve the above-mentioned functionalities in the prosthesis, a spring-based series-elastic actuation unit arranged around a hinge joint was incorporated into the design [7], [10]. The presence of compliance in the actuation system allows for greater impact-force absorption capability during walking, while simultaneously increasing the acceptable response period and decreasing the peak power requirement from the prime mover.

B. DESIGN SELECTIONS

Figures 2 and 3 show the CAD render and the schematic of the designed transtibial prosthesis, made of a foot and an actuated ankle joint. The system consists of the motor along with its shaft, the timing belt along with the set of gears, the ball screw along with the nut, and the yoke around the ball screw containing two springs. The foot-blade is attached to the yoke using a pin-joint. The power is injected into the ankle joint by the motor at specific instances based on the control architecture. This power is then transmitted to a ball screw (Misumi BSSCK1204) using the timing belt (Misumi S2M) and a high torque timing pulley set (Misumi S3M).
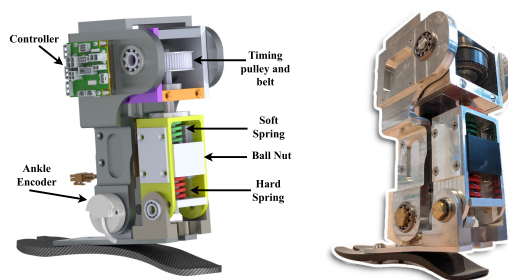

FIGURE 2. (left) A CAD render of the transtibial prosthesis showing the series elastic springs, ball screw, and timing belt mechanism integrated into the main design. The 3D drawings of all parts were made using Solidworks 2020 (Dassault Systèmes, France, www.solidworks.com). (right) The manufactured transtibial prosthesis.
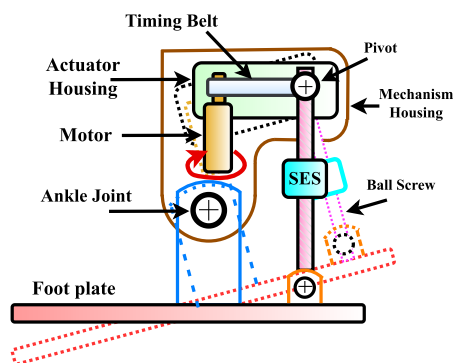

FIGURE 3. Schematic of the transtibial prosthesis showing the motor, timing belt mechanism, and series elastic springs mounted on the ball screw and held together by the mechanism housing. The dotted position represents the dorsiflexed ankle joint when the rotation of the ball screw compresses the series springs turning the foot plate about the ankle joint and the actuator housing around the pivot.
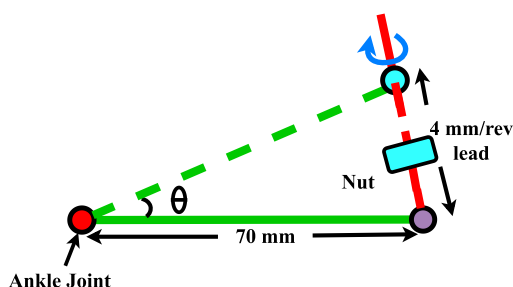

FIGURE 4. Geometry of the joint to determine the operation limits of the joint. The chosen motor rotates the nut with a lead of 4mm/rev, covering a distance of 61.89mm per second in the vertical direction, generating an angle θ of 41.48° about the horizontal in one second, fulfilling waking speed requirement of approximately 1 gait cycle per second.

As it can be observed from Figures 2, the clockwise rotation of the motor results in the rotation of the coupled ball screw. This rotation causes the ball-nut to slide upwards as the screw is not allowed to move axially, which causes plantarflexion of the foot, or when the motion is resisted causes a plantarflexion moment by compressing the spring (represented by green color), moving the entire yoke (shown in yellow color) upwards until it makes contact with the fixture. This satisfies the first functional requirement of the

prosthesis for a powered push-off. In contrast, a counterclockwise motor causes a dorsiflexion motion and/or leads to a dorsiflexing ankle moment by compression of the bottom spring(shown in red) leading to the return of the foot to a neutral position, satisfying the second functional requirement of the prosthesis. Figure 3 presents both the neutral and plantar-flexed positions of the ankle-foot system with respect to the other components. The detailed specifications of the components used in the design are outlined in Table 1.

TABLE 1. Specifications for the transtibial prosthesis components (motor, gears, timing belt, and pulleys).

Parameter	Ankle Joint
Motor Peak Power (W)	175 (approx)
Motor Voltage (V)	24
Motor Nominal Speed (rpm)	6870
Motor Torque constant (mNm/A)	28.6
Motor Torque (Stall) (mNm)	1800
Motor Thermal Time Constant (s)	32.7
Motor Gear Ratio	3.7:1
Ball Screw Lead (mm)	4
Ball Screw Max Load Dynamic (N)	2800
Ball Screw Shaft Outer diameter (mm)	12
Timing Belt Teeth Count	85
Timing Pulley Ratio	2:1
Timing Pulley Teeth Count (Gear/Pinion)	60/30

The selection of the ball screw was done by basing the calculations on the schematic shown in Figure 4. The linear force F required by the ball screw to provide the required torque (1.8 Nm/kg) for push-off about the ankle joint is calculated by using the horizontal distance (70 mm) from the pivot and the mass of the subject (70 kg) as follows:

$$F = \left(\frac{70 \text{ (kg)} \cdot 1.8 \text{ (Nm/kg)} \cdot 1000}{70 \text{ mm}} \right) = 1800 \text{ N} \quad (1)$$

By choosing a safety factor of 1.5, a ball screw was selected with a dynamic load carrying capacity of 2800N. The selection of the motor was based on the requirement of walking speed for the application. For our application, we chose reference walking speeds with a gait cycle time of 0.986 s, and having an angular range of $\approx 25°$s [36]. For our application, we choose a high torque 175 W motor with a nominal speed of 6870 rpm, coupled through a gear and timing belt reduction of $3.7 \cdot 2$. Using a ball screw with a lead of 4mm/rev and being actuated using the geared actuator, the distance D traveled by the screw in one second is given by:

$$D = \left(\frac{6870}{60 \cdot 3.7 \cdot 2} \right) \cdot 4 \text{ (mm/rev)} = 61.89 \text{ mm} \quad (2)$$

On the other hand, the angle θ traversed by the screw about the ankle joint in one second, acting from a distance of 70 mm is given by:

$$\theta = \tan^{-1}(D/70 \text{ mm}) = 41.48° \quad (3)$$

This angle is greater than the maximum ranges of ankle angle $\sim 25°$ s for one gait cycle, as shown in Figure 1. Hence, our selected high-torque motor is expected to be capable of

delivering the required ankle angular velocity for achieving walking speeds up to one gait cycle per second.

The system contains two springs to serve dual purposes. A relatively soft compression spring (length of 25 mm, stiffness of 100 N/mm, and load capacity of 1000 N) is meant to decrease the peak in-rush current for the motor and ensure a gradual build-up of torque before the application of the power-pulse during push-off. Adding the soft spring to the system allows for a longer response time along with reduced heat generated in the motor coils. A stiffer compression spring (length of 25 mm, stiffness of 375 N/mm, and load capacity of 2800 N) is active during the instances of heel strike, with the main objective of absorbing the impact that the joint experiences as the foot comes into contact with the ground. During the heel strike, the upward reaction force of the body weight is applied directly to the yoke through the heel of the foot-blade. At this point in the gait cycle, while the motor is holding the nut stationary, the upward force and plantarflexion motion of the foot compresses this spring against the ball nut and absorbs the impact of the heel strike, fulfilling the third functional requirement of the prosthesis.

The foot blade is a commercially available component, provided by Össur (Össur hf., Iceland, www.ossur.com).

III. CONTROL SYSTEM DESIGN

A. OBSERVATIONS

To develop the controller, we initiated the analysis by collecting data from an IMU placed on the tibia of a healthy male individual (height 175 cm, weight 60 kg) walking on a predefined course on level ground. The course was designed to capture data during the initiation and termination of the gait as well as during normal walking at self-selected comfortable speeds. The course consisted of 10 rounds of walking in a 25 m straight-line path before performing 180° turn and walking back 25 m.

Figure 5 shows the angular accelerations and angular velocities over 15 gait cycles as recorded during the above-mentioned experiments, by using the shank IMU (specifically from its triple-axis accelerometer and the gyroscope). The colored regions represent the data during gait initiation (red), normal walking (blue), and turning (yellow). From the plot, the following observations can be made: (i) The accelerometer data exhibits little repeatability in the +X (forward) and +Z (transverse) axes, while repetitions and reference points may be detected in the +Y (upwards) axis due to a separation between the crests and troughs. However, due to the nature of the data in the Y axis throughout the gait cycle, it is difficult to directly utilize the Y accelerometer data alone to uniquely identify the stance and swing phases of the gait. To use the Y accelerometer data for this characterization, it is possible to couple it with an oscillator of variable phase and frequency, as shown in our previous work [37]. However, since changes to the oscillator parameters require at least a couple of gait cycles, an alternative control method is investigated in this study. (ii) Secondly, the gyroscope data

exhibits a much wider range of angular velocities (between $+100$ and $-250°/s$) and a repetitive pattern maintained throughout the gait cycle in the $+Z$ axis. Taking turns shows a significant change in the magnitude of the data in the Y axis. This wider range and the presence of distinct regions of stance (0% to 60%) and swing phases (60% to 100%) in the $+Z$ direction make it possible to use the Z axis gyroscope data alone to identify the stance and swing phases of the gait.

By exploiting this possibility, a correlation between the tibial Z gyroscope data and the states of gait progression has been devised to design the control system for a transtibial prosthesis.
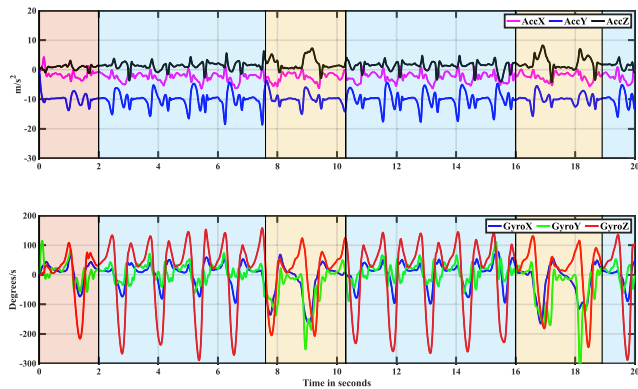

FIGURE 5. The accelerations and angular velocities of the tibia along three axes(X- forward, Y- towards gravity, Z- cross product of X and Y) of a healthy subject during level ground walking at a self-selected comfortable walking speed, recorded as a part of the experiments and used to determine the cut-off thresholds for the controller. Regions in red represent gait initiation, in blue normal walking, and in yellow left-side turnings.

B. CONTROLLER DESIGN

The development of the controller, which only uses the $+Z$ gyroscope data, involves a systematic approach consisting of three primary steps.

- The first step entailed identifying strategic events in the gyroscope data of one complete gait cycle that display minimal variation across multiple gait cycles and over a range of walking speeds. For this, 15 walking trials with straight line walking including left and right turns were conducted by the subject at self selected walking speeds. An average of all trials were taken to identify the control points. This procedure was performed only once for the subject. Figure 6 illustrates the four strategic control points identified, namely the reset step point (A), step detect point (B), stance rollover point (C), and power injection point (D).
- The second step was to segment the gyroscope data of one complete gait cycle based on the previously identified strategic control points. The offsets and cut-off points for each gait segment were determined by computing the mean and standard deviation over 10 gait cycles and inspecting them for consistent segmentation over multiple trials. This process was also performed only once for the subject. The reset step point A was

placed at a negative threshold crossing of $-100°/s$, the step detect point B at a threshold crossing of $65°/s$, the stance rollover point C at a threshold crossing of $35°/s$, and the power injection point D at a threshold crossing of $50°/s$.

- Finally, to provide a smooth transition between gait segments over multiple gait speeds, the velocity and acceleration of the motor during a gait segment (MV_{Gseg}) is determined by relating the step times recorded during the previous gait cycle(T_{prev}), the standard walking step time (T_{std}), and the motor speed for the standard walking (MV_{Gstd}). The standard values are obtained from [36] and applied to gait segments where motion is to be generated. Thus, for the motion dependant gait segments during each gait cycle the following set of equations applies:

$$scaling\_factor = T_{std}/T_{prev}$$
$$MV_{Gseg} = MV_{Gstd}/scaling\_factor$$

The velocity and acceleration initialization for the first step was performed using a pre-selected values from a healthy human gait cycle [36].
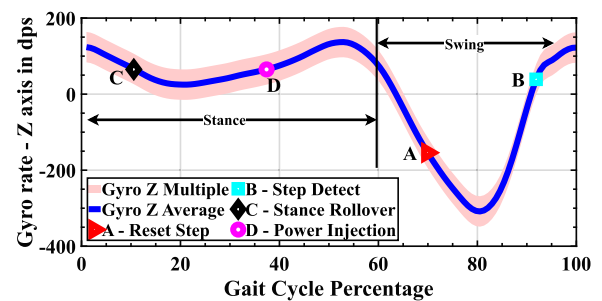

FIGURE 6. The figure shows a representation of the spread of gyro rate data of 15 trials(in pink) and their mean in degrees per second (°/s) with a standard deviation of $25°/s$ and variance of 5. The curve has been divided to identify strategic control points determining states of progression within a gait cycle.

Figure 7 provides an overview of the control architecture designed to govern the operation of the transtibial prosthesis, which comprises four stages beginning at A, that include reset-step detection, step detection, stance rollover, and power injection. The gait cycle time is calculated by determining the time difference between two consecutive step detect points B. This gait cycle time is then compared with the reference healthy human gait data [36] to determine the requisite motor velocities and accelerations for each subsequent gait cycle segment. The updated velocities and acceleration parameters, in conjunction with predetermined ankle joint positions for each segment, are then applied as motion references in the following cycle. The controller includes a time window for tallying the total number of steps, which must occur within this preset time frame to be considered valid. If no step is detected within the specified duration, the controller reverts to the reset point A, directing the prosthesis to return to a neutral ankle position.
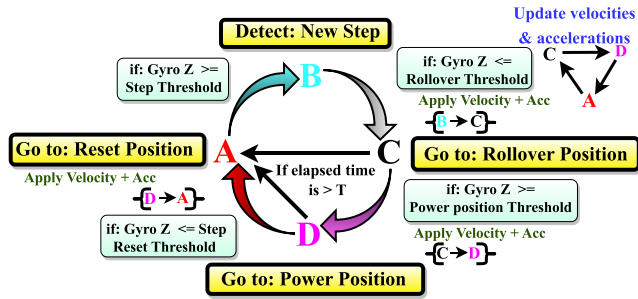
FIGURE 7. The overall control architecture of the prosthesis. The entire gait cycle is divided into four stages, which have been set via thresholds on the gyroscope data. The velocities and accelerations of the motor of the transtibial prosthesis are calculated using temporal data at the beginning of every gait cycle.

C. HARDWARE AND SOFTWARE ARCHITECTURE

The control system hardware comprises a Maxon EC-i 30 motor, a Maxon EPOS4 motion controller (Maxon Group, Switzerland, www.maxongroup.com), RM44 encoders (RLS, Slovenia, www.rls.si) that are positioned on the motor shaft and the ankle joint for position feedback, and a MPU9250 IMU (Sparkfun, USA, www.sparkfun.com) that is located on the tibia. The software algorithms run on a quad-core Raspberry Pi Zero 2W, and the operating system is Linux (Raspbian). Motion commands are transmitted from the Raspberry Pi to the controller using a USB serial communication protocol, and the sensors are read through an open-source implementation of a Raspberry Pi's I2C protocol. The system is powered by a 24V lab bench Base Tech BT-305 power supply.

The sampling rate for the IMU is fixed at 100 Hz, while the motor controller samples the hall sensors for the current sensing and the joint encoders for position feedback at a frequency of 25 kHz and 2.5 kHz, respectively. The pulse-width-modulation frequency for the controller is fixed at 50kHz and a Profile Position Mode (PPM, according to CiA402 CANopen Standards) has been used in sending commands to the motor controller. The IMU includes an onboard signal processor for data filtration using a low-pass filter whose cut-off frequency was set to 10Hz. The gyroscope signals from the IMU are further filtered in real-time using a 2nd order Butterworth filter with a cut-off frequency of 5Hz. The two-step data filtration introduces a delay of about 10ms in the signal processing.

The primary application software controlling the transtibial prosthesis was written in C++. Since the device is intended to be used for medical applications, real-time response with a maximum latency of 10ms was targeted. To improve the controller response, a real-time scheduling policy was chosen for the application. Highest priority was given to the application task, and it was set up to run isolated on core 2 of the processor. These changes ensured a predictable and deterministic response from the controller application.

IV. EXPERIMENTS

The experiments conducted for validating the control architecture involved a comprehensive analysis of various factors

such as the optimal selection of the sensor data rate, data filter coefficients, sensor placement around the tibia of a healthy participant, and sensor axial alignments to achieve accurate angular velocity curves that match the reference data set [36]. The experimental procedure, consisted of 20 trials conducted over multiple days with the same healthy male subject (as mentioned in section III), that entailed attaching the IMU around the tibia, enabling the subject to initiate and terminate the gait cycle at their preferred speed and timing. Self-selected walking speed and pattern were employed to derive more generalizable cut-off limit values compared to imposing a specific speed/pattern on the subject. The cut-off points and offsets for the control system were derived by taking an average over the first 5 trials and subsequently programmed into the control software. Once determined using pilot trials, these values were kept fixed for the rest of the experiments.[1]
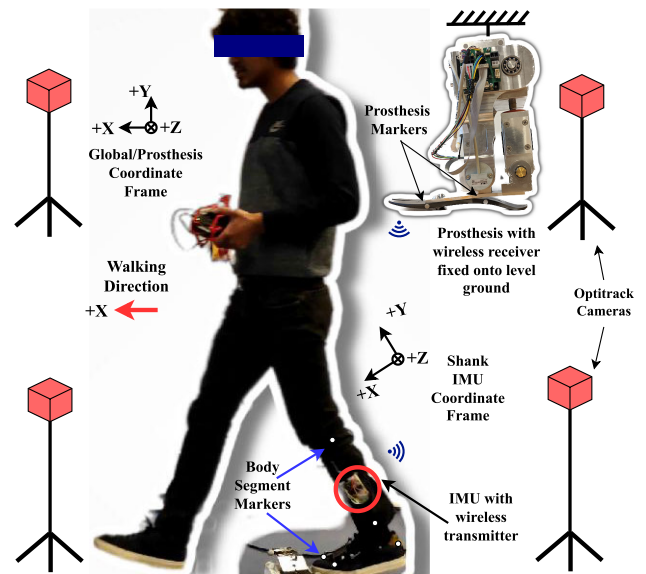

FIGURE 8. Experimental set-up for the validation of the proposed control architecture. Wireless data from the IMU are send directly to the prosthesis fixed in space using an attachment, while the prosthesis' angle and the ankle' angle were recorded using a motion capture system. The coordinate system configured as per International Society of Biomechanics (ISB) are also shown [38].

Figure 8 shows the experimental set-up for the validation of the control algorithm proposed in this study. The IMU was configured so that its $+X$ axis faces the direction of walking, the $-Y$ axis points downwards (direction of gravity). The angular velocity of the tibia about the $+Z$ axis is used as the control signal.

For all trials, the prosthesis was held fixed on a table using clamps, which allowed the prosthesis to perform its motion using wireless signals, without the need of being placed on the subject. To facilitate the testing process, a second IMU having the same characteristic and orientation as that of the IMU on

---

[1]The study, under protocol number M22.298663, was evaluated and received a waiver by the Medical Ethics Review Committee of the University Medical Center Groningen (Groningen, The Netherlands) on June 9, 2022.

the prosthesis, was worn on the tibia of the subject (prosthesis IMU was disabled), and the data were sent in real-time to the controller wirelessly. The motion of the prosthesis, the IMU data, and the actual tibia angles were determined using an OptiTrack (Natural Point Inc,USA, www.optitrack.com) motion capture system in real-time.

The experiments consisted of a walking trajectory in a 20*m* by 20*m* area where the subject (the same subject as the preliminary test) performed 10 rounds of normal walking in a straight line path while taking 180° turns to change directions. Following this, for the subsequent 10 rounds, the subject was asked to alter his walking pace between slow and fast walking in order to evaluate the performance of the controller during change of speed situations. Markers were placed on the subjects' foot and shank to generate body segments from which segment angles were calculated offline. Markers were also placed on the prosthesis in order to obtain the angle about the ankle joint, as shown in Figure 8.

The state of the gait was determined by the walking data received from the IMU attached to the tibia, and the required foot motion (plantarflexion/dorsiflexion) was directed to the actuator by the controller based on the walking velocity.

V. RESULTS

Figure 9 (top) shows the mean and standard deviation over a gait cycle of the results of the trials performed with the subject and the transtibial prosthesis. The top plot shows the subject's actual ankle angle captured with the motion tracking system (in blue) as compared to the prosthesis' ankle joint coming from the designed controller. Figure 9 (bottom) shows the tibia's angular velocity as recorded by the gyroscope placed around the tibia of the subject.
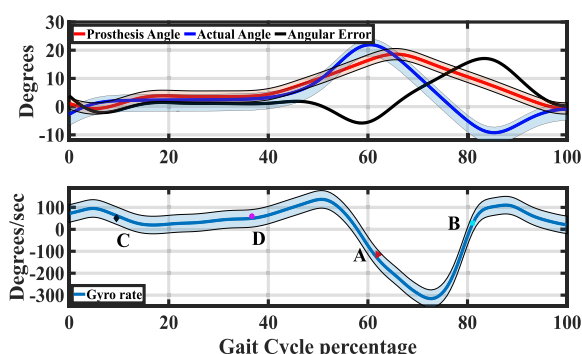

FIGURE 9. Subjects' ankle angle vs ankle angle of the prosthesis generated during real-time walking on level ground (above) and corresponding gyroscope data from the tibia IMU (below). The angular error between the prosthesis and actual angles have also been shown. The ankle angle has a maximum deviation of 5° and the gyro rates have a maximum deviation of 20°/*s*. Points C and D are the stance rollover and power injection points, whereas points A and B represent the reset and step detection points, respectively.

From the figure, it can be noted that, based on the IMU data, the prosthesis is capable of following the natural trajectory of the healthy human ankle joint to an extent. There is a greater degree of correlation between the actual

and the prosthetic angles from 10% to 50% (with almost no error encountered between the actual and prosthesis angles) of the gait cycle. Beyond the 50%, the relation diverges, with the actual ankle angle forming a crest at around 60% (error of −5°) followed by a trough around 85% (maximum error of 15°). Beyond this, the actual ankle angle reaches a neutral point by the end of the gait cycle. On the other hand, the prosthesis' ankle joint angle reaches its crest much later at around 65 − 70% of the gait cycle, and directly slopes to the neutral angle with the depression delayed and happening much later into the gait cycle. This discrepancy can be attributed to the fact that the final two stages of the gait cycle occur rapidly, whereas the controller's response and the maximum speed of the actuation system time is slower than required.

In Figure 9, a significant portion of the stance phase (between 10% to 35% of the gait cycle), the angle requested by the control algorithm only slightly changes. As a result, it is easier for the actuation system to maintain a match between the requested and actual prosthetic angle. Additionally, while a large change in joint angle and angular velocity is requested as soon as the power injection point D is detected, the actuation system accelerates towards the requested position. Although there is limited time between points D and A, the actuation system performs well and achieves a moderate degree of match between the requested and actual angle.

VI. DISCUSSION & OUTLOOK
A. DISCUSSION
The outcomes depicted in Figure 9, demonstrates that a prosthetic system can be designed utilizing a single sensor to meet the primary objective of level ground walking. A few aspects regarding the nature of this controller are discussed in the following paragraphs.

- The utilization of inertial sensors, as implemented in this study, demonstrates their efficacy of a single degree of freedom sensor in providing meaningful detection during the prosthesis's motion, mainly in the swing phase. The present configuration of a singular IMU sensor, positioned on the tibia, effectively detects limb motions throughout the gait cycle. Figure 9 indicates minimal variance of the gyroscope rate during the stance phase, leading to a control system's dependence on a sufficient separation between the strategic control points C and D while still rendering a reliable outcome. In some instances, the current division of the gait cycle into four parts may lead to slight jerks due to inexact matches of velocities between the loaded phases of. To avoid this, a suggestion on further subdividing the gait cycle may be made. This change, if needed, has to be introduced with care, due to the lack of presence of multiple extremum of angular rate (see Figure 6) that may be exploited effectively for this purpose.
- Another unique characteristic of the proposed control architecture is its ability to enable the system to actuate

seamlessly, even with variations in step times between two steps. This introduces a degree of freedom to for the user to walk at self selected speeds by removing restrictions that tied him/her to walk at discreetly controlled speeds. This in turn also aids through gait transitions from slow to medium and fast walking. The process by which the required motor speed during a gait segment was calculated by dividing the standard gait-segment speed by the ratio of standard gait cycle time [36] to the time taken by the subject during the previous gait cycle, ensured the possibility of an infinitely varying gait speed. In the current implementation, the determination of whether the subject is at rest or walking is achieved by counting the number of steps taken with the prosthesis [37]. As long as the step count remains 0, the prosthesis is considered to be at rest, and the controller maintains a neutral angle. As the user begins to walk and new steps are detected, the prosthesis is considered to be in motion, and the controller applies the requested motion patterns to the actuator. In order to activate the system, the subject must take at least one unassisted step, beyond which assistance is provided. When the subject takes only a single step, such as when moving in a confined space, the current logic while considering the prosthesis to be stationary provides only passive support through a neutral ankle joint.

The above mentioned controller was tested for multiple trials where the subject varied his gait speed during level ground walking while taking turns along the designed walking trajectory. The discussion and the results highlight the potential of this single DOF controller in facilitating prosthesis control. Moreover, as has been previously shown in [36], normal human gait patterns during level ground walking vary within set ranges of maximums and minimums. This suggests that the controller with little adjustments and knowledge of extremes of the walking pattern, can be generally used by a varied range of subjects and is robust enough for level ground walking applications. With further refinements, such a controller could serve as a foundation for application to a wider set of activities.

B. OUTLOOK

The implemented control technique on being verified for level ground walking with varying speeds may be refined by devising a method of addressing the change in error beyond the 50% mark in Figure 9. There are at least three possible techniques through which this may be achieved:

- The first approach entails modifying the offset of the power injection point D to ensure earlier detection in the gait cycle. By doing so, the actuation of the motor would have more time to react. However, given that the gyroscope data of the strategic control points C and D, as illustrated in Figure 9, are in close proximity to one another, any offset modifications must be carried out with due consideration for the potential for collusion between the two points. Furthermore,

the implementation of the instantaneous derivative of the signal in conjunction with the actual signal for detecting points C and D may yield advantageous results for the controller. The practical application of such modifications must take into account the placement of sensors and the variability of gyroscope data.

- The second approach involves reducing the offset for the reset step point A to approximately $-140°$/s. Lowering the offset from its current value, which is around $-100°$/s as depicted in Figure 9, would shift point A to the right, causing the reset to occur later in the gait cycle, potentially allowing for a longer period for motor actuation. However, decreasing the value of point A excessively may also result in a higher minimum walking velocity required for the system to operate without malfunction. Given that the minimum angular rate for slower walks can fall to $-150°$/s, setting the offset below this value could lead to missed reset points and unstable controller performance.

- Finally, enhancing the response characteristics of the joint involves utilizing a prime mover with superior speed and power properties. The implementation of a higher speed actuation system should enable the ankle joint to swiftly and accurately track the requested positions without any associated positional delays.

VII. LIMITATIONS

In this study, we attempted at determining the range of prosthesis-control-action of a controller that utilizes a single DOF sensor unit only. In this process, we developed the controller and the mechanical system to understand the limits of such a controller. Further enhancements in approach may be brought about in a couple of ways. In designing the prosthesis, we used a ball screw with a low coefficient of friction ($\eta = 0.92$) allowing the ankle to flex even in a non-powered situation. For safety purposes, it is suggested to either choose a ball screw with a lower efficiency or a lead screw with sufficient load ratings to prevent system back-drive-ability. This can potentially act as a safety mechanism for situations such as system power failure. Additionally, in the low-level controller for the system, a profile position mode (PPM) has been used for motor operation. In this mode, the target position values is directly provided along with the maximum values of current, torques, and accelerations, and an embedded trajectory generator determines the intermediate values according to pre-defined conventions. We feel that for closer tracking, a cyclic synchronous position mode (CSPM) could be used, which enables a finer control of the actuator by reducing delays and instantaneously passing information of torques, positions, velocities, and accelerations to the controller.

The current method suggests that it is capable of controlling a transtibial prosthesis during level ground walking, however, domains such as ascending/descending stairs, ascending/descending ramps, very high-speed walking, and other activities of daily living are not covered by it. In these

cases, the magnitudes of the gyroscope rates are usually different compared to that of level ground walking. The cut-off thresholds chosen in the current implementation might not accurately map to these cases. To use the proposed control architecture for non-level ground walking, studies on the relations between angular velocity and angles, need to be performed. However, to accommodate the diverse demands of everyday life, we recommend further testing with multiple subjects with multiple gait patterns across varied situations. This would help create a comprehensive solution that is well-suited to meet the needs of a larger user base.

Finally, in order to further enhance the system's performance and ensure even greater user-confidence on the controller, a secondary information pipeline (example through additional sensory input) to continuously update or maintain inter gait step velocities and accelerations could be added to the proposed control architecture. Fortunately, impedance controlled strategies [7], [10] provide an effective solution to this challenge by leveraging either a force/torque sensor or pre-determined limb segment masses to model external forces. This method leads to the adjustment of ankle joint impedance and admittance, which in turn could enhance the system performance and user comfort.

VIII. CONCLUSION

In this work, we have explored the potential of using a single sensor to control a transtibial prosthesis for variable walking speeds. The implemented single DOF controller, having verified across multiple trials, has provided a foundation for basic control during level ground walking, with a potential for greater advancements in the future. While currently the testing is limited to a single subject over multiple days, due to the inherent simplicity in its design we are optimistic that the controller with little to no adjustments will be robustly suitable for other subjects undergoing level ground walking with turns. This controller thus offers possibilities for enhancing prosthesis control for real-life applications and daily activities. Overall, our work demonstrates great potential for improving the quality of life of individuals using powered prostheses.

ACKNOWLEDGMENT

REFERENCES

[1] N. T. Pickle, J. M. Wilken, J. M. Aldridge, R. R. Neptune, and A. K. Silverman, "Whole-body angular momentum during stair walking using passive and powered lower-limb prostheses," *J. Biomech.*, vol. 47, no. 13, pp. 3380–3389, Oct. 2014.

[2] M. J. Major and N. P. Fey, "Considering passive mechanical properties and patient user motor performance in lower limb prosthesis design optimization to enhance rehabilitation outcomes," *Phys. Therapy Rev.*, vol. 22, nos. 3–4, pp. 202–216, Jul. 2017.

[3] M. A. Price, P. Beckerle, and F. C. Sup, "Design optimization in lower limb prostheses: A review," *IEEE Trans. Neural Syst. Rehabil. Eng.*, vol. 27, no. 8, pp. 1574–1588, Aug. 2019.

[4] F. Barberi, E. Anselmino, A. Mazzoni, M. Goldfarb, and S. Micera, "Toward the development of user-centered neurointegrated lower limb prostheses," *IEEE Rev. Biomed. Eng.*, vol. 17, pp. 212–228, 2024.

[5] M. Tschiedel, M. F. Russold, and E. Kaniusas, "Relying on more sense for enhancing lower limb prostheses control: A review," *J. NeuroEng. Rehabil.*, vol. 17, no. 1, pp. 1–13, Dec. 2020.

[6] R. Gehlhar, M. Tucker, A. J. Young, and A. D. Ames, "A review of current state-of-the-art control methods for lower-limb powered prostheses," *Annu. Rev. Control*, vol. 55, pp. 142–164, Apr. 2023.

[7] S. K. Au, J. Weber, and H. Herr, "Powered ankle-foot prosthesis improves walking metabolic economy," *IEEE Trans. Robot.*, vol. 25, no. 1, pp. 51–66, Feb. 2009.

[8] H. A. Varol, F. Sup, and M. Goldfarb, "Multiclass real-time intent recognition of a powered lower limb prosthesis," *IEEE Trans. Biomed. Eng.*, vol. 57, no. 3, pp. 542–551, Mar. 2010.

[9] R. Unal, F. Klijnstra, S. M. Behrens, E. E. G. Hekman, S. Stramigioli, H. F. J. M. Koopman, and R. Carloni, "The control of recycling energy strorage capacity for WalkMECHadapt," in *Proc. 23rd IEEE Int. Symp. Robot Human Interact. Commun.*, Aug. 2014, pp. 720–725.

[10] F. Sup, "A powered self-contained knee and ankle prosthesis for near normal gait in transfemoral amputees," Ph.D. dissertation, Dept. of Mech. Eng., Vanderbilt Univ., Nashville, TN, USA, 2009.

[11] B. E. Lawson, B. Ruhe, A. Shultz, and M. Goldfarb, "A powered prosthetic intervention for bilateral transfemoral amputees," *IEEE Trans. Biomed. Eng.*, vol. 62, no. 4, pp. 1042–1050, Apr. 2015.

[12] M. Li, Y. Wen, X. Gao, J. Si, and H. Huang, "Toward expedited impedance tuning of a robotic prosthesis for personalized gait assistance by reinforcement learning control," *IEEE Trans. Robot.*, vol. 38, no. 1, pp. 407–420, Feb. 2022.

[13] F. Zhang and H. Huang, "Source selection for real-time user intent recognition toward volitional control of artificial legs," *IEEE J. Biomed. Health Informat.*, vol. 17, no. 5, pp. 907–914, Sep. 2013.

[14] F. Sup, H. Varol, J. Mitchell, T. Withrow, and M. Goldfarb, "Design and control of an active elctrical knee and ankle prosthesis," in *Proc. IEEE RAS/EMBS Int. Conf. Biomed. Robot. Biomechatronics*, Oct. 2008, pp. 523–528.

[15] D. Xu, S. Crea, N. Vitiello, and Q. Wang, "Online estimation of continuous gait phase for robotic transtibial prostheses based on adaptive oscillators," in *Proc. IEEE/ASME Int. Conf. Adv. Intell. Mechatronics (AIM)*, Jul. 2020, pp. 1890–1895.

[16] R. D. Gregg, T. Lenzi, L. J. Hargrove, and J. W. Sensinger, "Virtual constraint control of a powered prosthetic leg: From simulation to experiments with transfemoral amputees," *IEEE Trans. Robot.*, vol. 30, no. 6, pp. 1455–1471, Dec. 2014.

[17] D. J. Villarreal and R. D. Gregg, "A survey of phase variable candidates of human locomotion," in *Proc. 36th Annu. Int. Conf. IEEE Eng. Med. Biol. Soc.*, Aug. 2014, pp. 4017–4021.

[18] S. Rezazadeh, D. Quintero, N. Divekar, E. Reznick, L. Gray, and R. D. Gregg, "A phase variable approach for improved rhythmic and non-rhythmic control of a powered knee-ankle prosthesis," *IEEE Access*, vol. 7, pp. 109840–109855, 2019.

[19] D. L. Grimes, W. C. Flowers, and M. Donath, "Feasibility of an active control scheme for above knee prostheses," *J. Biomech. Eng.*, vol. 99, no. 4, pp. 215–221, Nov. 1977.

[20] D. L. Grimes, "An active multi-mode above knee prosthesis controller," Ph.D. dissertation, Dept. of Mech. Eng., Massachusetts Inst. Technol., Cambridge, MA, USA, 1979.

[21] G. W. Horn, "Electro-control: Am EMG-controlled A/K prosthesis," *Med. Biol. Eng.*, vol. 10, no. 1, pp. 61–73, Jan. 1972.

[22] C. D. Hoover and K. B. Fite, "Preliminary evaluation of myoelectric control of an active transfemoral prosthesis during stair ascent," in *Proc. ASME Dyn. Syst. Control Conf. (DSCC)*, vol. 1, 2010, pp. 801–808, doi: 10.1115/DSCC2010-4158.

[23] F. Zhang, M. Liu, and H. Huang, "Preliminary study of the effect of user intent recognition errors on volitional control of powered lower limb prostheses," in *Proc. Annu. Int. Conf. IEEE Eng. Med. Biol. Soc.*, Aug. 2012, pp. 2768–2771.

[24] K. S. Türker, "Electromyography: Some methodological problems and issues," *Phys. Therapy*, vol. 73, no. 10, pp. 698–710, Oct. 1993.

[25] R. Merletti, M. Aventaggiato, A. Botter, A. Holobar, H. Marateb, and T. M. M. Vieira, "Advances in surface EMG: Recent progress in detection and processing techniques," *Crit. Rev. Biomed. Eng.*, vol. 38, no. 4, pp. 305–345, 2010.

[26] M. Duvinage, T. Castermans, and T. Dutoit, "Control of a lower limb active prosthesis with eye movement sequences," in *Proc. IEEE Symp. Comput. Intell., Cognit. Algorithms, Mind, Brain (CCMB)*, Apr. 2011, pp. 1–7.

[27] L. Mutlu, E. Uyar, O. Baser, and L. Cetin, "Modelling of an under-hip prosthesis with ankle and knee trajectory control by using human gait analysis," *IFAC Proc.*, vol. 44, no. 1, pp. 9668–9673, Jan. 2011.

[28] R. Ronsse, N. Vitiello, T. Lenzi, J. van den Kieboom, M. C. Carrozza, and A. J. Ijspeert, "Adaptive oscillators with human-in-the-loop: Proof of concept for assistance and rehabilitation," in *Proc. 3rd IEEE RAS EMBS Int. Conf. Biomed. Robot. Biomechatronics*, Sep. 2010, pp. 668–674.

[29] S. Heins, L. Flynn, H. Laloyaux, J. Geeroms, D. Lefeber, and R. Ronsse, "Compliant control of a transfemoral prosthesis by combining feed-forward and feedback," in *Proc. 8th IEEE RAS/EMBS Int. Conf. Biomed. Robot. Biomechatronics (BioRob)*, Nov. 2020, pp. 452–458.

[30] A. A. Alzaydi, A. Cheung, N. Joshi, and S. Wong, "Active prosthetic knee fuzzy logic-pid motion control, sensors and test platform design," *Int. J. Sci. Eng. Res.*, vol. 2, no. 12, pp. 1–17, Dec. 2011.

[31] J. Lim, "The mechanical design and analysis of an active prosthetic knee," M.S thesis, Dept. Mech.Eng., Univ. Waterloo, Waterloo, ON, USA, 2008.

[32] M. A. Holgate, T. G. Sugar, and A. W. Bohler, "A novel control algorithm for wearable robotics using phase plane invariants," in *Proc. IEEE Int. Conf. Robot. Autom.*, May 2009, pp. 3845–3850.

[33] M. Grimmer, "Powered lower limb prostheses," Ph.D. dissertation, Dept. of Mech. Eng. and Dept. of Hum. Movement Sci., Tech. Univ. Darmstadt, Darmstadt, Germanny, 2015.

[34] D. Quintero, D. J. Villarreal, D. J. Lambert, S. Kapp, and R. D. Gregg, "Continuous-phase control of a powered knee–ankle prosthesis: Amputee experiments across speeds and inclines," *IEEE Trans. Robot.*, vol. 34, no. 3, pp. 686–701, Jun. 2018.

[35] R. D. Gregg, E. J. Rouse, L. J. Hargrove, and J. W. Sensinger, "Evidence for a time-invariant phase variable in human ankle control," *PLoS ONE*, vol. 9, no. 2, Feb. 2014, Art. no. e89163.

[36] D. A. Winter, *Biomechanics Motor Control Human Movement*. Hoboken, NJ, USA: Wiley, 1990.

[37] A. Mazumder, E. E. G. Hekman, and R. Carloni, "An adaptive hybrid control architecture for an active transfemoral prosthesis," *IEEE Access*, vol. 10, pp. 52008–52019, 2022.

[38] G. Wu and P. R. Cavanagh, "ISB recommendations for standardization in the reporting of kinematic data," *J. Biomech.*, vol. 28, no. 10, pp. 1257–1261, Oct. 1995.

ANIKET MAZUMDER received the B.Tech. degree in mechanical engineering from the West Bengal University of Technology (WBUT), and the M.Tech. degree in mechanical engineering from the Indian Institute of Technology (IIT), Gandhinagar, India, in 2017. He is currently pursuing the Ph.D. degree with the Faculty of Science and Engineering, Bernoulli Institute of Mathematics, Computer Science and Artificial Intelligence, University of Groningen. His primary research interests include the characterization of human gait, design and control of prosthetic systems, and the development of sensor fusion algorithms and applications.

EDSKO E. G. HEKMAN (Member, IEEE) received the B.Sc. degree in liberal arts and engineering from the Calvin College, Grand Rapids, MI, USA, and the Ingenieur (Master of Science) degree from the Delft University of Technology, in 1986. He has developed instrumentation for research with the Radboud University of Nijmegen, for some years. After that, he accepted a position as an Assistant Professor with the Department of Biomechanical Engineering, University of Twente. His research areas are the development of assistive devices (orthotics, prosthetics, and exoskeletons) and endoprosthetics for the spine.

RAFFAELLA CARLONI (Senior Member, IEEE) received the M.Sc. degree in electronic engineering from the University of Bologna, Italy, and the Ph.D. degree from the Department of Electronics, Computer Science and Systems, University of Bologna. She was an Assistant Professor/an Associate Professor with the University of Twente, Enschede, The Netherlands, from 2008 to 2017. She joined the University of Groningen, The Netherlands, in 2017, where she is currently an Associate Professor with the Faculty of Science and Engineering, Bernoulli Institute for Mathematics, Computer Science and Artificial Intelligence. Her research interests include design, modeling, and control of compliant robotic systems; novel (soft) actuators; and prosthetic devices.

● ● ●